Systematic Control of the Packing Density of Self-Assembled Monolayers Using Bidentate and Tridentate Chelating Alkanethiols

Joon-Seo Park, Andy Nguyen Vo, David Barriet, Young-Seok Shon,† and T. Randall Lee*

Department of Chemistry, University of Houston, 4800 Calhoun Road, Houston, Texas 77204-5003

Received October 2, 2004. In Final Form: December 22, 2004

The structural and interfacial properties of self-assembled monolayers (SAMs) on gold derived from the adsorption of a series of 1,1,1-tris(mercaptomethyl)alkanes (i.e., $CH_3(CH_2)_mC[CH_2SH]_3$, where $m = 9$, 11, 13, 15) were investigated. The new SAMs, which possess uniformly low densities of alkyl chains, were characterized by ellipsometry, contact angle goniometry, and polarization modulation infrared reflection absorption spectroscopy. Additional analysis of the SAMs by X-ray photoelectron spectroscopy permitted a direct calculation of the packing densities of the SAMs on gold. The results as a whole, when compared to those obtained on SAMs generated from normal alkanethiols ($CH_3(CH_2)_{m+2}SH$), 2-alkylpropane-1,3-dithiols ($CH_3(CH_2)_mCH[CH_2SH]_2$), and 2-alkyl-2-methylpropane-1,3-dithiols ($CH_3(CH_2)_mC(CH_3)[CH_2SH]_2$) having analogous chain lengths, demonstrate that the 1,1,1-tris(mercaptomethyl)alkanes afford SAMs with alkyl chains having the lowest packing density and least conformational order.

Introduction

Self-assembled monolayers (SAMs) have been widely investigated for the past two decades due to their potential use in a number of technologies, including those involving adhesion, wetting, corrosion prevention, and lubrication.[1] Furthermore, the applications of SAMs have been expanding into emerging areas, such as nanoelectronics[2] and biosensors.[3] The widespread interest in and use of SAMs can be attributed in part to their densely packed and highly ordered structures. In particular, the macroscopic surface properties of semicrystalline SAMs are dictated by their microscopic structure and composition. Thus, the interfacial properties of densely packed and highly ordered SAMs are predictable and readily controlled through the use of specific chain lengths and tailgroups.[1]

Loosely packed and thus conformationally disordered SAMs have received relatively little attention from interfacial scientists. Our research group, however, believes that the conformational flexibility of alkyl chains in loosely packed SAMs offers distinct characteristics that can lead to unique technological applications. For example, SAMs having a low density of alkyl chains can be used to control thrombus formation on the surface of biomedical devices.[4] Because thrombus formation through protein adsorption on surfaces is a critical obstacle in the development of biocompatible devices,[5] much research has been carried out to prepare surfaces that are resistant to protein adsorption.[6−9] One strategy for controlling protein adsorption is to deposit or grow a protective layer of protein, such as human serum albumin (HSA), on surfaces to prevent the adsorption of other blood proteins.[4] Foster and co-workers investigated the effect of the packing density of SAMs on HSA adsorption.[4,10] These researchers observed that HSA bound more tenaciously to loosely packed SAMs than to densely packed SAMs due to the penetration of HSA into the loosely packed SAMs. Another application of loosely packed SAMs involves reversibly switching surfaces, which were reported by Langer and co-workers.[11] Prior to Langer's work, attempts to control the in situ structure of densely packed SAMs had been unsuccessful due to relatively strong van der Waals interactions between chains, especially when long chain alkanethiols were employed.[12] In contrast, the flexibility of alkyl chains in loosely packed SAMs, arising from void space between the chains, led to reversible changes in interfacial properties in response to an electrical potential.[11]

Although loosely packed SAMs are beginning to find intrinsic technological applications, the quantitative control of packing density remains a challenge to this field of research. Excluding our approach involving chelating adsorbates (vide infra), at least four methodologies have been employed to prepare loosely packed SAMs. Low packing densities of alkyl chains have been achieved via the coadsorption of two or more adsorbates having different chain lengths.[13−16] This method provides a useful tool to

* To whom correspondence should be addressed. E-mail: trlee@uh.edu.

† Current address: Department of Chemistry, Western Kentucky University, Bowling Green, KY 42101.

(1) Ulman, A. *Chem. Rev.* **1996**, *96*, 1533.

(2) Ishida, T. In *Chemistry of Nanomolecular Systems*: *Towards the Realization of Molecular Devices*; Springer Series in Chemical Physics, Vol. 70; Springer: Berlin, 2003; p 91.

(3) Chaki, N. K.; Vijayamohanan, K. *Biosens. Bioelectron.* **2002**, *17*, 1.

(4) Choi, E. J.; Foster, M. D.; Daly, S.; Tilton, R.; Przybycien, T.; Majkrzak, C. F.; Witte, P.; Menzel, H. *Langmuir* **2003**, *19*, 5464.

(5) *Biomaterials Science*: *An Introduction to Materials in Medicine*; Ratner, B. D., Hoffman, A. S., Schoen, F. J., Lemons, J. E., Eds.; Academic: San Diego, CA, 1996.

(6) Wang, R. L. C.; Kreuzer, H. J.; Grunze, M. *J. Phys. Chem. B* **1997**, *101*, 9767.

(7) Harder, P.; Grunze, M.; Dahint, R.; Whitesides, G. M.; Laibinis, P. E. *J. Phys. Chem. B* **1998**, *102*, 426.

(8) Feldman, K.; Haehner, G.; Spencer, N. D.; Harder, P.; Grunze, M. *J. Am. Chem. Soc.* **1999**, *121*, 10134.

(9) Pertsin, A. J.; Grunze, M.; Garbuzova, I. A. *J. Phys. Chem. B* **1998**, *102*, 4918.

(10) Choi, E. J.; Foster, M. D. *Langmuir* **2002**, *18*, 557.

(11) Lahann, J.; Mitragotri, S.; Tran, T.-N.; Kaido, H.; Sundaram, J.; Choi, I. S.; Hoffer, S.; Somorjai, G. A.; Langer, R. *Science* **2003**, *299*, 371.

(12) Schoenfisch, M. H.; Pemberton, J. E. *Langmuir* **1999**, *15*, 509.

(13) Bain, C. D.; Whitesides, G. M. *Science* **1988**, *240*, 62.

10.1021/la0475573 CCC: $30.25
Published on Web 03/05/2005

control the surface composition by adjusting the ratio of mixed adsorbates. The coadsorption, however, can lead to phase segregation ("islanding") if the adsorbates are quite different in their chemical functionalities and/or structures.[14,16] In the case of mixed normal alkanethiol SAMs, phase segregation at room temperature has been observed when the chain length difference is larger than four carbon atoms.[16] In addition, the composition and thus the packing density of adsorbates having long alkyl chains cannot be easily predicted from the composition of mixed alkanethiol solutions; for example, depending on the experimental conditions, the preferential adsorption of one adsorbate is typically observed.[14]

An alternative strategy for preparing loosely packed SAMs is based on the use of unsymmetrical disulfides.[17−19] A critical drawback of this method is that the surface composition and/or packing density cannot be controlled systematically. Furthermore, this strategy can potentially lead to phase segregation and/or preferential loss of one of the components because dialkyl disulfides are known to dissociate upon adsorption.[20] Although unsymmetrical sulfides can be used to avoid the problems related to dissociation, one study has reported that SAMs generated from sulfides are markedly less stable than those generated from alkanethiols.[21]

An intriguing approach for preparing loosely packed SAMs was recently reported.[11] The self-assembly of a 16-mercaptohexadecanoic acid (MHA) derivative possessing a bulky endgroup (2-chlorophenyldiphenylmethyl group) followed by cleavage of the endgroup was used to generate a low density MHA SAM. Although this method appears to offer control over the packing density of the resulting SAMs by varying the steric bulk of endgroups of the adsorbates, the authors have yet to demonstrate this capability. Moreover, current adsorbates are restricted to alkanethiols possessing acid-labile endgroups, leading exclusively to hydrophilic surfaces exposing carboxylate moieties. This limitation might prevent the general use of this strategy in the preparation of loosely packed SAMs. The low packing density near sulfur headgroups also might lead to unstable monolayers due to diminished chain−chain interactions.

A fourth strategy for preparing loosely packed SAMs employs a relatively short equilibration time of substrates in adsorbate solutions. The immersion of silicon wafers into a hexadecyltrichlorosilane solution for 30 s was used to generate relatively loosely packed SAMs, while immersion for 5 h led to densely packed monolayers.[4] Given, however, that the generally accepted two-step adsorption mechanism involves the formation of islands at the initial stage of SAM formation (the fast regime),[22] this strategy probably affords inhomogeneous surfaces in the loosely packed regime.

The development of a general method for preparing well-defined loosely packed SAMs is one of our major research objectives. In previous work,[23] our group has prepared loosely packed SAMs via the adsorption of the chelating 2-monoalkylpropane-1,3-dithiols (**C*n*C2**, Figure 1). The resulting liquidlike organic films exhibited substantially enhanced wettabilities and frictional properties when compared to densely packed analogues prepared from normal alkanethiols (**C*n***).[23−25] Furthermore, the chelating alkanedithiols provided enhanced stabilities to the resulting SAMs due to the chelate effect and the energetically disfavored formation of cyclic disulfide and/or multimolecular desorption products.[26] We also have demonstrated that unsymmetrical chelating alkanedithiols can be used to prepare homogeneously mixed SAMs at the molecular level.[27] In further efforts to control the packing density, we prepared a series of 2-alkyl-2-methylpropane-1,3-dithiols (**C*n*C3**) that possessed methyl groups near the quaternary carbon center.[28] Due to the steric bulk of the methyl group, the SAMs derived from **C*n*C3** exhibited even lower packing densities than those derived from **C*n*C2**.

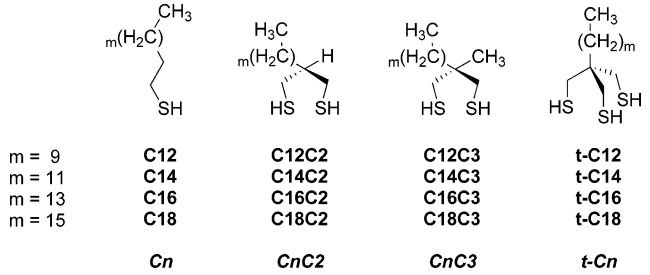

Figure 1. Structures of the adsorbates: normal alkanethiols (**C*n***), 2-monoalkylpropane-1,3-dithiols (**C*n*C2**), 2-alkyl-2-methylpropane-1,3-dithiols (**C*n*C3**), and 1,1,1-tris(mercaptomethyl)alkanes (**t-C*n***).

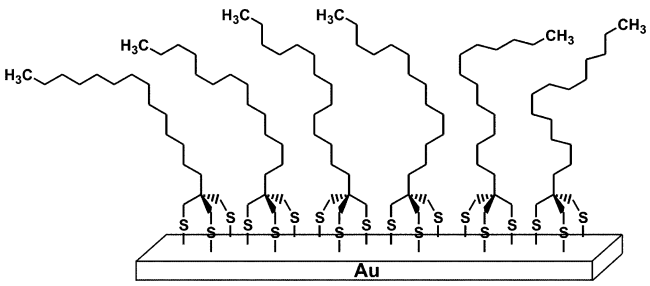

Figure 2. Schematic representation of a conformationally disordered SAM having a low packing density of alkyl chains (**t-C16**).

In this report, we describe a new series of loosely packed SAMs generated from the tridentate chelating alkanethiols, 1,1,1-tris(mercaptomethyl)alkanes (**t-C*n***, Figures 1 and 2). We anticipated that the SAMs derived from **t-C*n*** would exhibit a lower packing density of alkyl chains than those derived from the bidentate analogues due to the low alkyl-to-sulfur ratio of **t-C*n*** (1:3) relative to those of **C*n*C2** and **C*n*C3** (1:2). We also anticipated that the **t-C*n*** adsorbates would generate thermodynamically more stable SAMs than the bidentate chelating alkanethiols because of an enhanced chelate effect. Furthermore, we

(14) Bain, C. D.; Whitesides, G. M. *J. Am. Chem. Soc.* **1989**, *111*, 7164.
(15) Bain, C. D.; Whitesides, G. M. *Angew. Chem.* **1989**, *101*, 522.
(16) Chen, S.; Li, L.; Boozer, C. L.; Jiang, S. *Langmuir* **2000**, *16*, 9287.
(17) Biebuyck, H. A.; Bain, C. D.; Whitesides, G. M. *Langmuir* **1994**, *10*, 1825.
(18) Higashi, N.; Takahashi, M.; Niwa, M. *Langmuir* **1999**, *15*, 111.
(19) Niwa, M.; Morikawa, M.-a.; Nabeta, T.; Higashi, N. *Macromolecules* **2002**, *35*, 2769.
(20) Biebuyck, H. A.; Whitesides, G. M. *Langmuir* **1993**, *9*, 1766.
(21) Troughton, E. B.; Bain, C. D.; Whitesides, G. M.; Nuzzo, R. G.; Allara, D. L.; Porter, M. D. *Langmuir* **1988**, *4*, 365.
(22) Xu, S.; Cruchon-Dupeyrat, S. J. N.; Garno, J. C.; Liu, G.-Y.; Jennings, G. K.; Yong, T.-H.; Laibinis, P. E. *J. Chem. Phys.* **1998**, *108*, 5002.
(23) Shon, Y.-S.; Colorado, R., Jr.; Williams, C. T.; Bain, C. D.; Lee, T. R. *Langmuir* **2000**, *16*, 541.
(24) Lee, S.; Shon, Y.-S.; Colorado, R., Jr.; Guenard, R. L.; Lee, T. R.; Perry, S. S. *Langmuir* **2000**, *16*, 2220.
(25) Shon, Y.-S.; Lee, S.; Colorado, R., Jr.; Perry, S. S.; Lee, T. R. *J. Am. Chem. Soc.* **2000**, *122*, 7556.
(26) Shon, Y.-S.; Lee, T. R. *J. Phys. Chem. B* **2000**, *104*, 8192.
(27) Shon, Y.-S.; Lee, S.; Perry, S. S.; Lee, T. R. *J. Am. Chem. Soc.* **2000**, *122*, 1278.
(28) Park, J.-S.; Smith, A. C.; Lee, T. R. *Langmuir* **2004**, *20*, 5829.

expected that the **t-C*n*** adsorbates would provide homogeneously distributed alkyl chains across the surface as reported for the dithiol systems. Consequently, the tridentate chelating alkanethiols (**t-C*n***) can be used in conjunction with the **C*n*C2** and **C*n*C3** adsorbates to control the packing density of alkyl chains on surfaces in a systematic fashion.

This paper describes the synthesis of 1,1,1-tris(mercaptomethyl)alkanes (**t-C*n***) and their use in the preparation of loosely packed SAMs on gold. The SAMs were characterized by ellipsometry, contact angle goniometry, polarization modulation infrared reflection−absorption spectroscopy (PM-IRRAS), and X-ray photoelectron spectroscopy (XPS). The data were compared with those obtained from SAMs generated via the adsorption of normal alkanethiols (**C*n***), 2-monoalkylpropane-1,3-dithiols (**C*n*C2**), and 2-alkyl-2-methylpropane-1,3-dithiols (**C*n*C3**) to demonstrate their relative packing densities and interfacial structure and properties.

Experimental Section

Materials and Methods. Gold shot (99.99%) was obtained from Americana Precious Metals, and test-grade polished single-crystal silicon(111) wafers were purchased from NESTEC. Aqueous formaldehyde (36.5−38.0%), potassium hydroxide (KOH), triethylamine (Et_3N), sodium bicarbonate ($NaHCO_3$), methylene chloride (CH_2Cl_2), hexanes, anhydrous diethyl ether, and tetrahydrofuran (THF) were purchased from EM Sciences; THF was dried by passage through activated alumina before use. Normal alkanethiols, starting 1-hydroxyalkanes, dimethyl sulfoxide (DMSO), and diethyl malonate were purchased from Aldrich Chemical Co.; DMSO was dried over calcium hydride and then distilled and stored under argon. Lithium aluminum hydride (LAH) and magnesium sulfate ($MgSO_4$) were obtained from Alfa Aesar and Fisher Scientific Co., respectively. Pyridinium chlorochromate was prepared using a route reported by Corey and Suggs.[29] Methanesulfonyl chloride and potassium thioacetate (KSAc) were purchased from Acros, and absolute ethanol was purchased from Aaper Alcohol and Chemical Co. and used as received. Column chromatography was performed using Natland International silica gel, 60−200 mesh. Thin-layer chromatography (TLC) was performed using 200-μm-thick silica gel plates purchased from Sorbent Technologies. An iodine chamber was used to analyze the eluted TLC plates because most compounds were not visible under UV light (254 nm). ^{1}H and ^{13}C nuclear magnetic resonance (NMR) spectra were recorded on a General Electric QE-300 spectrometer operating at 300 and 75 MHz for ^{1}H and ^{13}C nuclei, respectively. The spectra were obtained in chloroform-*d* purchased from Cambridge Isotope Laboratories, and chemical shifts were referenced relative to the residual proton or carbon signal of the deuterated solvent (δ 7.26 for ^{1}H and δ 77.00 for ^{13}C spectra).

Synthesis of Chelating Alkanethiol Adsorbates. The 1,1,1-tris(mercaptomethyl) alkanes (**t-C*n***) were prepared using the strategy outlined in Scheme 1. The starting aldehyde **1** for the Tollens condensation was synthesized by oxidation of the corresponding alcohol by pyridinium chlorochromate.[29] To prepare the key intermediate, 1,1,1-tris(hydroxymethyl)alkane **2**, we employed a Tollens condensation, which proceeds via two steps: aldol condensation of formaldehyde with an aldehyde followed by a Canizzaro reduction.[30,31] After purification of the crude **2** by triturating in diethyl ether, treatment of the resulting white powder with methanesulfonyl chloride and triethylamine readily afforded the 1,1,1-tris(methanesulfonyloxymethyl)alkane **3**.

As an illustrative example, we provide below detailed procedures for the synthesis of 1,1,1-tris(mercaptomethyl)heptadecane (**t-C18**). We also provide complete analytical data for all other **t-C*n*** adsorbates, including ^{1}H and ^{13}C NMR spectra (see Supporting Information). Please note that the products often contained trace amounts of the corresponding disulfides, and the reaction conditions were not optimized to improve the overall yield. Also, previous reports have described the synthesis and characterization of the 2-monoalkylpropane-1,3-dithiol (**C*n*C2**) and the 2-alkyl-2-methylpropane-1,3-dithiol (**C*n*C3**) adsorbates.[23,28]

Scheme 1

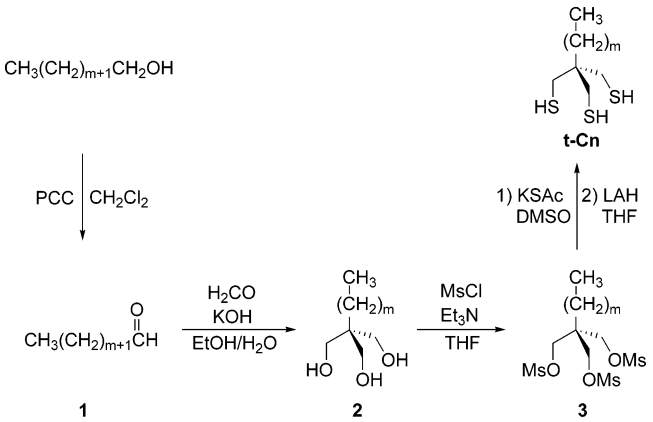

*Octadecanal (**1**).*[29] Pyridinium chlorochromate (26.67 g, 123.7 mmol) was suspended in 100 mL of anhydrous CH_2Cl_2. To the stirred suspension was added a solution of 1-octadecanol (20.00 g, 73.94 mmol) in CH_2Cl_2. Stirring was continued for 3 h at room temperature, and the black chromium compounds were removed by passage through a short pad of silica gel. The filtrate was concentrated to dryness and purified by column chromatography on silica gel (hexanes) affording octadecanal (15.00 g, 55.87 mmol; 76%). ^{1}H NMR (300 MHz, $CDCl_3$): δ 9.76 (t, J = 1.5 Hz, 1 H, C(O)*H*), 2.42 (dt, J = 1.5 Hz, 7.2 Hz, 2 H, C*H*$_2$C(O)), 1.58 (m, 2 H, C*H*$_2$CH$_2$C(O)), 1.38−1.20 (m, 28 H), 0.85 (t, J = 6.7 Hz, 3 H, C*H*$_3$).

*1,1,1-Tris(hydroxymethyl)heptadecane (**2**).*[30] Octadecanal (8.10 g, 30.2 mmol) and aqueous formaldehyde (36.5−38.5%, 20 mL, excess) were dissolved in 50 mL of aqueous ethanol (50%). To this stirred mixture was added a solution of potassium hydroxide (3.40 g, 60.1 mmol) in 50 mL of aqueous ethanol (50%). The reaction mixture was stirred for 4 h at room temperature and heated to 60 °C for 5 h. The ethanol was removed by rotary evaporation, and the residue was extracted with diethyl ether (3 × 100 mL). The combined organic phases were washed with water (3 × 100 mL), dried over $MgSO_4$, and concentrated to dryness. The crude products were triturated in diethyl ether and filtered to give a white powder (2.90 g, 8.77 mmol; 29%). ^{1}H NMR (300 MHz, $CDCl_3$): δ 3.76 (s, 6 H, C*H*$_2$OH), 2.39 (br s, 3 H, O*H*), 1.40−1.12 (m, 30 H), 0.88 (t, J = 6.7 Hz, 3 H, C*H*$_3$).

*1,1,1-Tris(methanesulfonyloxymethyl)heptadecane (**3**).* Triol **2** (2.28 g, 6.90 mmol) and triethylamine (2.80 g, 27.7 mmol) were placed in 75 mL of THF under argon. To the stirred solution was added dropwise methanesulfonyl chloride (3.20 g, 27.9 mmol) over 5 min. Stirring of the reaction mixture was continued at room temperature for 4 h under argon. Ice-cold water (50 mL) was poured into the flask to destroy any remaining methanesulfonyl chloride. The mixture was extracted with diethyl ether (3 × 100 mL). The combined organic phases were washed with dilute HCl (1 × 100 mL), water (1 × 100 mL), $NaHCO_3$ solution (1 × 100 mL), and water (1 × 100 mL). The organic layer was dried over $MgSO_4$, filtered, and concentrated to dryness to afford crude 1,1,1-tris(methanesulfonyloxymethyl)heptadecane (3.50 g, 6.20 mmol; 90%). ^{1}H NMR (300 MHz, $CDCl_3$): δ 4.16 (s, 6 H, C*H*$_2$OMs), 3.07 (s, 9 H, O*Ms*), 1.38−1.19 (m, 30 H), 0.88 (t, J = 6.7 Hz, 3 H, C*H*$_3$).

*1,1,1-Tris(mercaptomethyl)heptadecane (**t-C18**).* The crude product **3** (1.97 g, 3.49 mmol) was dissolved in dry DMSO (20 mL). After potassium thioacetate (2.91 g, 25.5 mmol) was added to the stirred solution, the reaction mixture was heated to 130 °C for 24 h under an atmosphere of argon. Water (75 mL) was poured into the solution, and the mixture was extracted with diethyl ether (3 × 100 mL). During extractions, sodium chloride was added to the mixture to facilitate phase separation. The combined organic phases were washed with brine (3 × 100 mL),

(29) Corey, E. J.; Suggs, J. W. *Tetrahedron Lett.* **1975**, 2647.
(30) Weibull, B.; Matell, M. *Acta Chem. Scand.* **1962**, *16*, 1062.
(31) Hu, J.; Mattern, D. L. *J. Org. Chem.* **2000**, *65*, 2277.

dried over $MgSO_4$, and filtered. After the solvent was removed by rotary evaporation, the crude product was placed in THF (20 mL), and LAH (1.50 g, 39.5 mmol) was added slowly at room temperature. The reaction mixture was refluxed for 4 h under an atmosphere of argon and then quenched by slow addition of ethanol (25 mL). The mixture was acidified by careful addition of 1 M HCl solution (150 mL) and then extracted with diethyl ether (3 × 100 mL). The combined organic layers were washed with dilute HCl solution (2 × 100 mL) and brine (1 × 100 mL). The organic phase was dried over $MgSO_4$ and filtered. After removal of the volatiles by rotary evaporation, the crude product was purified by column chromatography on silica gel (hexanes/diethyl ether, 1/0→20/1) to afford 1,1,1-tris(mercaptomethyl)-heptadecane (white powder, 0.45 g, 1.2 mmol; 34%). ^{1}H NMR (300 MHz, $CDCl_3$): δ 2.58 (d, J = 8.7 Hz, 6 H, SCH_2), 1.38−1.16 (m, 30 H), 1.17 (t, J = 8.7 Hz, 3 H, S*H*), 0.88 (t, J = 6.9 Hz, 3 H, CH_3). ^{13}C NMR (75 MHz, $CDCl_3$): δ 41.38, 32.43, 31.93, 30.10, 30.05, 29.67, 29.53, 29.37, 29.27, 29.06, 23.27, 22.70, 14.14.

*1,1,1-Tris(mercaptomethyl)undecane (**t-C12**).* ^{1}H NMR (300 MHz, $CDCl_3$): δ 2.58 (d, J = 8.4 Hz, 6 H, SCH_2), 1.37−1.15 (m, 18 H), 1.17 (t, J = 8.4 Hz, 3 H, S*H*), 0.88 (t, J = 6.9 Hz, 3 H, CH_3). ^{13}C NMR (75 MHz, $CDCl_3$): δ 41.38, 32.44, 31.87, 30.10, 29.59, 29.51, 29.32, 29.07, 23.26, 22.67, 14.11.

*1,1,1-Tris(mercaptomethyl)tridecane (**t-C14**).* ^{1}H NMR (300 MHz, $CDCl_3$): δ 2.58 (d, J = 8.7 Hz, 6 H, SCH_2), 1.40−1.17 (m, 22 H), 1.17 (t, J = 8.7 Hz, 3 H, S*H*), 0.88 (t, J = 6.9 Hz, 3 H, CH_3). ^{13}C NMR (75 MHz, $CDCl_3$): δ 41.38, 32.44, 31.91, 30.11, 29.63, 29.51, 29.34, 29.08, 23.27, 22.69, 14.12.

*1,1,1-Tris(mercaptomethyl)pentadecane (**t-C16**).* ^{1}H NMR (300 MHz, $CDCl_3$): δ 2.58 (d, J = 8.1 Hz, 6 H, SCH_2), 1.39−1.17 (m, 26 H), 1.17 (t, J = 8.1 Hz, 3 H, S*H*), 0.88 (t, J = 6.9 Hz, 3 H, CH_3). ^{13}C NMR (75 MHz, $CDCl_3$): δ 47.53, 32.77, 31.92, 30.30, 29.64, 29.47, 29.36, 29.07, 23.27, 22.69, 14.13.

Preparation and Characterization of SAMs. Detailed procedures for the preparation of gold-coated silicon wafers and SAM formation have been provided in previous reports.[28] The gold substrates were immersed in solutions containing the specified adsorbates at 1 mM concentrations. For all chelating adsorbates, an adsorption/equilibration time of 48 h was used to generate SAMs having maximum coverages.[32] The instrumentation and methods employed to perform the ellipsometry, contact angle measurements, polarization modulation infrared reflection−absorption spectroscopy, and X-ray photoelectron spectroscopy have also been described.[28]

Results and Discussion

Throughout this article, we compare the SAMs generated from **t-C*n*** to those generated from **C*n***, **C*n*C2**, and **C*n*C3** that possess the same number of carbon atoms from the sulfur headgroup to the terminal methyl group in the primary (longer) chain (see Figure 1).

Effect of Solvent on the Formation of t-C*n* SAMs. Early studies by electron diffraction[33] and low energy helium diffraction[34] showed that the sulfur−sulfur spacing on the surfaces of SAMs generated from normal alkanethiols (**C*n***) is approximately 5 Å, with the sulfur atoms binding to the 3-fold hollow sites on Au(111) surfaces.[35] Molecular modeling of the 1,1,1-tris(mercaptomethyl)-pentadecane adsorbate (**t-C16**) shows, however, that the average distance between sulfur atoms in a single **t-C16** adsorbate is approximately 3.5 Å in a conformation in which the three sulfur atoms point in the same direction (e.g., toward a surface).[36] Given the structural constraints of the **t-C*n*** adsorbates, the potential for incomplete binding of sulfur atoms on gold must be considered. As mentioned above, we anticipated that the trithiols (**t-C*n***) would form more loosely packed SAMs on gold than normal alkanethiols (**C*n***) and dithiols (**C*n*C2** and **C*n*C3**) due to their low alkyl-to-sulfur ratio (1:3). Furthermore, we anticipated that the enhanced chelating effect of **t-C*n*** adsorbates would lead to more stable monolayers than the **C*n*C2** and **C*n*C3** SAMs as well as the **C*n*** SAMs. To realize these expectations, it is essential that all three sulfur atoms of a **t-C*n*** adsorbate bind to the surface of gold. We, therefore, sought to characterize the chemical state of the sulfur atoms in SAMs generated from **t-C*n*** on gold before further experimentation.

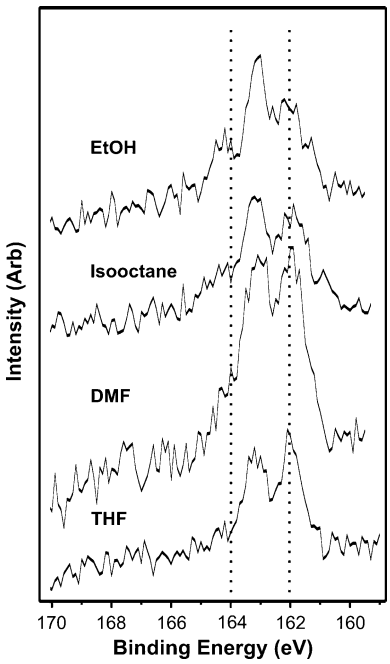

Figure 3. XPS spectra of the S_{2p} region for SAMs derived from 1,1,1-tris(mercaptomethyl)pentadecane (**t-C16**) in the indicated solvents.

The nature of sulfur−gold bonding in SAMs can be evaluated by monitoring the binding energies in XPS, because bonding influences the distribution of electrons in the atoms of interest.[37] Thus, the S_{2p} region of XPS spectra can provide evidence for bond formation between the sulfur headgroup and the gold substrate.[38,39] In XPS spectra of SAMs generated from alkanethiols on gold, the binding energy of the $S_{2p3/2}$ peak for thiols bound to gold is known to be 162 eV.[39] In contrast, the $S_{2p3/2}$ peak for unbound thiols appears roughly at 164 eV.[39] Incomplete adsorbate binding on gold, therefore, can be identified and quantified by the presence of the S_{2p} peak at 164 eV. Although the sulfur signal is significantly attenuated by overlying alkyl chains (leading to a low signal-to-noise ratio) and spin−orbit coupling can disturb an accurate analysis of the region, we believe that analysis of the $S_{2p3/2}$ peak is the most reliable method to evaluate the chemical nature of sulfur atoms in SAMs. Thus, we used XPS to characterize the SAMs generated from **t-C*n*** upon adsorption from various organic solvents (see Figure 3).

Ethanol is the most widely used solvent for preparing SAMs on gold. The popularity of ethanol can be attributed

(32) Shon, Y.-S.; Lee, T. R. *J. Phys. Chem. B* **2000**, *104*, 8182.
(33) Strong, L.; Whitesides, G. M. *Langmuir* **1988**, *4*, 546.
(34) Chidsey, C. E. D.; Liu, G. Y.; Rowntree, P.; Scoles, G. *J. Chem. Phys.* **1989**, *91*, 4421.
(35) Recent work by grazing incidence X-ray diffraction suggests, however, that the sulfur headgroups dimerize in the form of surface-bound disulfides: Fenter, P.; Eberhardt, A.; Eisenberger, P. *Science* **1994**, *226*, 1216.
(36) Molecular modeling was performed using AM1 semiempirical calculations with PC Spartan Plus, Wave function, Irvine, CA.
(37) *Surface Analysis: The Principal Techniques*; Vickerman, J. C., Ed.; Wiley: Chichester, 1997.
(38) Laibinis, P. E.; Whitesides, G. M.; Allara, D. L.; Tao, Y. T.; Parikh, A. N.; Nuzzo, R. G. *J. Am. Chem. Soc.* **1991**, *113*, 7152.
(39) Castner, D. G.; Hinds, K.; Grainger, D. W. *Langmuir* **1996**, *12*, 5083.

to its relatively low price, its availability in high purity, and its low toxicity. In addition, ethanol has a low tendency to be incorporated into SAMs.[40] Based on these considerations and the fact that ethanol is known to form robust and fully bound **C*n***, **C*n*C2**, and **C*n*C3** SAMs on gold,[28] we chose to employ ethanol as the solvent in initial probes of the formation of **t-C*n*** SAMs. The gold substrates were immersed in 1 mM ethanolic solutions of **t-C16** and allowed to equilibrate for 48 h. The slides were exhaustively rinsed with toluene and ethanol and then dried under a vigorous stream of ultrapure nitrogen before analysis by XPS. Unfortunately, the XPS spectra of the resulting **t-C16** SAMs reproducibly exhibited an S_{2p} peak at 164 eV, indicating incomplete binding of the adsorbate on gold. Apparently for these structurally strained adsorbates, solvation of the thiol groups through hydrogen bonding with ethanol disrupts the complete binding of the sulfur atoms.

We then explored the use of a nonpolar aprotic solvent, isooctane, for the formation of **t-C*n*** SAMs. However, XPS spectra of SAMs prepared similarly in isooctane also exhibited an S_{2p} peak at 164 eV, albeit with a markedly weaker intensity (see Figure 3). Although we cannot fully rationalize the incomplete binding of **t-C*n*** in isooctane, we reasoned that polar solvents might be required for complete binding of all three thiolates of **t-C*n*** if the mechanism of adsorption involves at least partial charge separation.[41] We therefore explored the use of polar aprotic solvents, such as dimethylformamide (DMF) and THF. Analysis by XPS of **t-C*n*** SAMs prepared in DMF still exhibited an S_{2p} peak at 164 eV, but the relative intensity of the peak (164 eV peak/162 eV peak) was smaller than those observed for the SAMs prepared in ethanol and isooctane. In contrast, the use of THF led to little or no peak at 164 eV, indicating that all (or nearly all) of the sulfur atoms in the **t-C*n*** SAMs are bound when prepared in THF. Consequently, we used THF as the solvent to prepare all **t-C*n*** SAMs for further characterization and evaluation. For the reasons outlined above, ethanol was used for all other adsorbates.

Ellipsometric Thickness. Ellipsometry is normally employed as one of the principle tools for the characterization of SAMs. From the ellipsometric thickness, the quality of a well-known SAM, such as that generated from a normal alkanethiol, can be evaluated, and the degree of coverage for a unique SAM can be estimated. For all of the organic monolayers prepared in this study, we assumed a value of 1.45 as the refractive index. Given, however, that the refractive index values might be substantially influenced by the surface coverage and/or chain length, the measured ellipsometric thicknesses should be always supported by other analytical data before drawing conclusions. Nevertheless, ellipsometry provides a convenient and powerful tool for preliminary evaluation of the relative degree of coverage of SAMs.

It is known that the alkyl chains in SAMs generated from normal alkanethiols (**C*n***) are fully trans extended and tilt 30° from the surface normal, maintaining a stabilizing interchain van der Waals distance of 4.2 Å.[1] We assume, however, that the alkyl chains in loosely packed SAMs are more tilted from the surface normal due to their diminished interchain van der Waals attraction and the void space between chains. As a result, loosely packed SAMs can be expected to exhibit lower ellipsometric thicknesses than their densely packed analogues. Furthermore, due to their enhanced interchain spacing, the alkyl chains in loosely packed SAMs are expected to possess a substantial number of gauche defects. For loosely packed SAMs, therefore, we will use the "average" tilt angle to describe the chain tilt because a single tilt angle cannot represent the actual state of all of the alkyl chains (see Figure 2). Figure 4 shows the ellipsometric thicknesses of the SAMs generated from all of the adsorbates examined in this study. The thicknesses of the SAMs generated from **t-C*n*** are ~8, 3, and 1 Å lower than those of the corresponding SAMs generated from **C*n***, **C*n*C2**, and **C*n*C3**, respectively. As noted above, a lower ellipsometric thickness suggests a lower packing density of alkyl chains and thus a higher average tilt angle. From the measured ellipsometric thicknesses, therefore, the relative packing densities of the SAMs can be estimated as follows: **C*n*** ≫ **C*n*C2** > **C*n*C3** > **t-C*n***. The relative packing densities of the SAMs estimated from ellipsometric thicknesses are identical to those expected on the basis of the structures of the adsorbates. Given, however, the alkyl-to-sulfur ratio of the adsorbates (1:1 for **C*n***, 1:2 for **C*n*C2** and **C*n*C3**, and 1:3 for **t-C*n***), the small difference in the ellipsometric thicknesses between the **C*n*C3** and **t-C*n*** SAMs is somewhat surprising. One possible explanation for such a small difference is that the structurally more constrained sulfur moieties in **t-C*n*** might allow a more densely packed monolayer with regard to the sulfur headgroups. This assumption, however, requires a more quantitative analysis of the packing density of the SAMs because the refractive index for **t-C*n*** SAMs might be markedly different from those for **C*n*C2** and **C*n*C3** SAMs as well as that for **C*n*** SAMs.

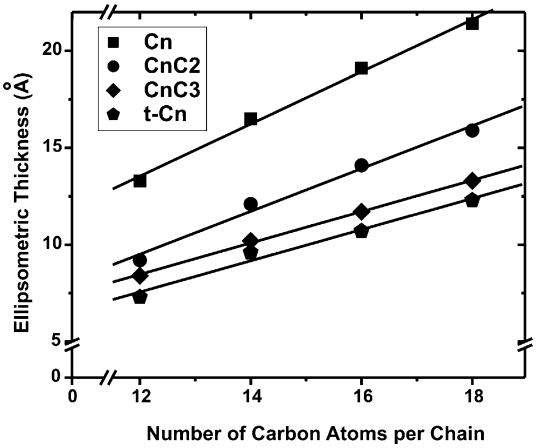

Figure 4. Ellipsometric thicknesses of SAMs derived from **C*n*** (squares), **C*n*C2** (circles), **C*n*C3** (diamonds), and **t-C*n*** (pentagons).

The average tilt angle of the alkyl chains can be estimated from the slopes shown in Figure 4. The slope in a plot of ellipsometric thickness versus the number of carbon atoms corresponds to the film thickness per methylene unit for each adsorbate. Bain and co-workers have reported a theoretical slope of 1.27 Å/CH_2 unit for **C*n*** SAMs using known bond angles and bond lengths and assuming fully trans extended monolayers tilted 30° from the surface normal.[40,42] Given that all of the adsorbates used in this research are saturated hydrocarbons and thus should have the same bond angles and bond lengths, a lower slope should represent a highly tilted monolayer and/or increased gauche defects. In Figure 4, the slope for

(40) Bain, C. D.; Troughton, E. B.; Tao, Y. T.; Evall, J.; Whitesides, G. M.; Nuzzo, R. G. *J. Am. Chem. Soc.* **1989**, *111*, 321.

(41) Carey, F. A.; Sundberg, R. J. *Advanced Organic Chemistry*, 3rd ed.; Plenum: New York, 1990.

(42) The following values were used to calculate the theoretical slope: C−C = 1.545 Å, ∠CCC = 110.5°, C−S = 1.81 Å, C−H = 1.1 Å, and contribution from S = 1.5 Å.

C*n* is 1.3 Å/CH_2, which is in good agreement with the theoretical slope as well as that reported previously by our group.[28] In contrast, the slopes for **C*n*C2**, **C*n*C3**, and **t-C*n*** are 1.1, 0.81, and 0.81 Å/CH_2, respectively. The data suggest that the average tilt angle of alkyl chains in the **t-C*n*** SAMs is substantially higher than that of the **C*n*** SAMs as well as those of the **C*n*C2** SAMs. The slope, however, for the **t-C*n*** SAMs is identical to that for the **C*n*C3** SAMs, suggesting similar average chain tilts for these two adsorbates.

Wettability. As an apolar aprotic contacting liquid, hexadecane has been widely employed to characterize hydrocarbon surfaces.[15,23] In particular, our group has demonstrated that hexadecane is a powerful tool for exploring the nanoscale conformation of loosely packed SAMs.[23,25,28] It is known that interfacial methylene groups are more wettable than interfacial methyl groups.[14,25,40,43] We have rationalized this phenomenon using an atomic contact model.[25,28] Densely packed and well-ordered SAMs derived from **C*n*** expose predominantly methyl groups at the surface, where the methyl−methyl spacing is ~5 Å.[33,34] In contrast, loosely packed SAMs expose a substantial fraction of methylene groups at the surface, and thus the surface consists of both methyl and methylene groups. Given that the C−C bond length in saturated alkyl chains is 1.54 Å, which is significantly shorter than the methyl−methyl spacing in densely packed SAMs (~5 Å), loosely packed SAMs expose a greater number of atomic contacts per unit area than do densely packed analogues. The higher density of atomic contacts enhances the van der Waals interactions between the surface and the contacting liquid, and thus enhances the wettability.[25,28]

Examination of Figure 5a reveals lower contact angles of hexadecane on the **t-C*n*** surfaces than on the **C*n*C2** and **C*n*C3** surfaces as well as the densely packed **C*n*** surfaces. According to the atomic contact model described above, the SAMs derived from **t-C*n*** apparently expose a higher fraction of methylene groups at the surface than those derived from **C*n*C2** and **C*n*C3** as well as **C*n***. From the observed wettabilities, therefore, the relative packing densities of the SAMs can be estimated in the following order: **C*n*** ≫ **C*n*C2** > **C*n*C3** > **t-C*n***.

Another interesting observation from Figure 5a is the dependence of the wettability on the chain length of the adsorbates in the loosely packed SAMs. For example, the contact angles of the densely packed SAMs derived from **C*n*** are largely independent of chain length. In contrast, the contact angles of hexadecane on the loosely packed SAMs (**C*n*C2**, **C*n*C3**, and **t-C*n***) progressively increase as a function of chain length. This chain length dependence can be rationalized on the basis of the following two hypotheses. First, for loosely packed SAMs, the degree of conformational order might increase with increasing chain length,[40,44] exposing a lesser fraction of methylene groups at the surface. Therefore, loosely packed SAMs having shorter alkyl chains exhibit enhanced wettabilities compared to those having longer alkyl chains. Second, the contacting liquid might interact through van der Waals forces with the underlying gold substrate due to the low film thicknesses of the loosely packed SAMs.[40] Because the van der Waals forces between the contacting liquid and the underlying gold substrate are greatest when the distance between them is the smallest,[40] loosely packed SAMs having shorter alkyl chains would be expected to be more wettable than those having longer alkyl chains.

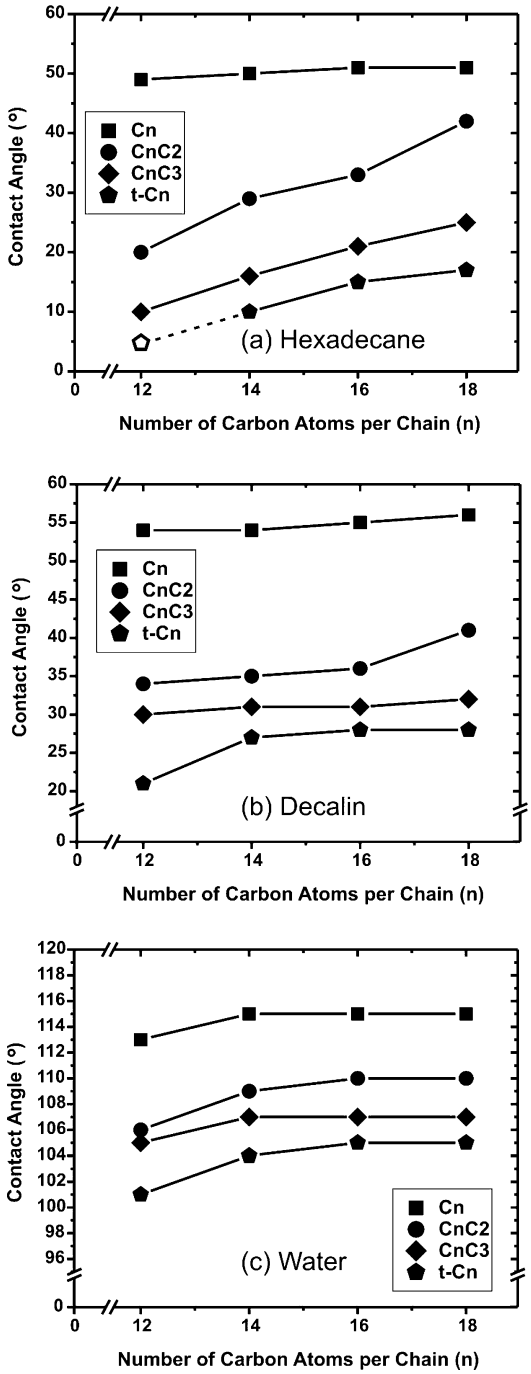

Figure 5. Advancing contact angles of (a) hexadecane, (b) Decalin, and (c) water on SAMs derived from **C*n*** (squares), **C*n*C2** (circles), **C*n*C3** (diamonds), and **t-C*n*** (pentagons). The SAM derived from **t-C12** was completely wet by hexadecane (θ_a < 10°).

Of these two hypotheses, the former is unsupported by the ellipsometric thickness measurements (and the IR data presented in a subsequent section). Specifically, the ellipsometric thicknesses for the loosely packed SAMs (**C*n*C2**, **C*n*C3**, **t-C*n***) increase linearly as a function of chain length. This linear dependence suggests that the degree of conformational order of the loosely packed SAMs (**C*n*C2**, **C*n*C3**, **t-C*n***) is roughly the same for all chain lengths examined in this research. The relatively invariant wettability of the **C*n*** series probably arises from the fact that the liquid is held at a sufficiently large distance from the surface for all chain lengths examined; hence, the van der Waals forces are small and largely inconsequential.[40] Given these considerations, we propose that the chain

(43) Chaudhury, M. K. *Mater. Sci. Eng., R* **1996**, *R16*, 97.
(44) Porter, M. D.; Bright, T. B.; Allara, D. L.; Chidsey, C. E. D. *J. Am. Chem. Soc.* **1987**, *109*, 3559.

Table 1. Contact Angle Hysteresis ($\Delta\theta$) of Hexadecane, Decalin, and Water on SAMs Derived from the Indicated Adsorbates[a]

	hexadecane				decalin				water			
	C12	C14	C16	C18	C12	C14	C16	C18	C12	C14	C16	C18
C*n*	6	6	6	6	5	5	5	5	10	11	10	10
C*n*C2	10	10	10	7	6	5	5	5	10	11	12	12
C*n*C3	–	–	10	10	5	5	5	5	10	11	11	12
t-C*n*	–	–	–	–	4	4	5	5	10	10	10	9

[a] We report values from at least three independent experiments, and values were reproducible within ±1° of those reported. Entries marked by (–) could not be measured because advancing and/or receding contact angles are less than 10°, which we define as fully wettable.

length dependence of the wettability of loosely packed SAMs arises from changes in the strength of the van der Waals interaction between the contacting liquid and the underlying gold substrate.

As shown in Figure 5a, the SAM derived from **t-C12** was completely wettable by hexadecane (θ_a < 10°). In addition, Table 1 shows that the contact angle hysteresis values ($\Delta\theta = \theta_a - \theta_r$) of hexadecane on the loosely packed bidentate SAMs (**C*n*C2** and **C*n*C3**; ~10°) are measurably larger than those of the densely packed analogues (**C*n***; 6°). Furthermore, the contact angle hysteresis of hexadecane on the SAMs derived from **t-C*n*** could not be determined because the receding angles on those SAMs were too low to be measured reliably.

It is known that the contact angle hysteresis is influenced by the heterogeneity of surfaces and by certain interactions between the surface and the liquid, such as the reorganization of surface molecules and the adsorption of contacting liquids.[45] Given that one of the major merits of our system is the formation of homogeneously distributed components, the increased hysteresis of hexadecane on the loosely packed SAMs should be evaluated carefully. We assume that hexadecane can intercalate into the loosely packed SAMs during the contact angle measurements due to the presence of void spaces between alkyl chains in those SAMs. The partially intercalated hexadecane might increase the interaction between hexadecane and the surfaces, and in turn decrease the receding contact angles increasing the magnitude of the contact angle hysteresis. To evaluate this hypothesis, we employed decalin (decahydronaphthalene) as an alternative contacting liquid because its steric bulk can inhibit intercalation into loosely packed SAMs. Furthermore, we anticipated that the contact angles of decalin would be higher than those of hexadecane due to its higher surface tension,[46] allowing the collection of receding contact angle data for all of the SAMs. As anticipated, we were able to collect receding contact angle data with decalin, which in turn gave low and constant contact angle hysteresis values (~5°) for the all of the SAMs examined (Table 1), indicating that the alkyl chains in the SAMs are homogeneously distributed across the surfaces. The constant hysteresis values observed for water (~10°; Table 1) further support the formation of homogeneous SAMs.

Although less pronounced than hexadecane, the contact angles of decalin and water were also observed to increase with increasing chain length (Figure 5b,c). Polar protic contacting liquids, such as water, are known to be highly sensitive to the presence of trace amounts of surface-confined polar species but largely insensitive to minor differences in nonpolar species because the liquids are highly self-associated through hydrogen bonding.[23,47] Nevertheless, water also exhibited a distinguishable decreasing trend in wettability with increasing chain length on the loosely packed SAMs (Figure 5c). As a whole, the observed wettabilities are in good agreement with the ellipsometric thicknesses, a fact which further confirms that the alkyl chain density and the conformational order of the SAMs decrease in the following order: **C*n*** ≫ **C*n*C2** > **C*n*C3** > **t-C*n***. We note, however, that loosely packed SAMs possessing well ordered and highly tilted alkyl chains can also exhibit significantly enhanced wettabilities and diminished ellipsometric thicknesses. For example, the alkyl chains in the SAMs derived from normal alkanethiols on GaAs(100) are highly ordered and tilted away from the surface normal by 57°, while the corresponding SAMs on gold possess a chain tilt angle of 30°.[48] Consequently, the normal alkanethiol SAMs on GaAs(100) exhibit a lower contact angle of hexadecane (41°) than the analogous SAMs on gold (~50°). The lower contact angle on GaAs can be rationalized on the basis of the partial exposure of underlying methylene units arising from the higher chain tilt. This comparison thus illustrates that wettability and ellipsometric thickness cannot provide an unequivocal measure of the degree of conformational order in organic thin films.

PM-IRRAS. The C–H stretching region of surface infrared spectra can be used to evaluate the orientation and conformational order of organic thin films.[23,28,49,50] In particular, the frequency and bandwidth of the methylene antisymmetric and symmetric bands ($\nu_a^{CH_2}$ and $\nu_s^{CH_2}$) are known to be strongly influenced by the conformational order of hydrocarbons, including organic monolayers.[44,51–53] For example, crystalline polyethylene exhibits a $\nu_a^{CH_2}$ band at 2920 cm^{-1} and a $\nu_s^{CH_2}$ band at 2850 cm^{-1}, while liquid polyethylene shows these bands at 2928 and 2856 cm^{-1}, respectively.[51] The same trend has been reported for normal alkanethiols: the $\nu_a^{CH_2}$ and $\nu_s^{CH_2}$ peaks of crystalline *n*-docosanethiol appear at 2918 and 2851 cm^{-1}, while those of liquid state *n*-octanethiol appear at 2924 and 2855 cm^{-1}.[44]

Figure 6 and Table 2 show the positions of the $\nu_a^{CH_2}$ and $\nu_s^{CH_2}$ bands for the SAMs generated from **C*n***, **C*n*C2**, **C*n*C3**, and **t-C*n***. Assignment of the C–H stretching bands is based on literature precedents.[28,49,50] The $\nu_a^{CH_2}$ and $\nu_s^{CH_2}$ bands for the **C*n*** SAMs appear at 2919 and 2851 cm^{-1}, respectively, indicating the crystalline-like conformational order of the alkyl chains. The loosely packed SAMs (**C*n*C2**, **C*n*C3**, and **t-C*n***) exhibited only small differences in $\nu_a^{CH_2}$ and $\nu_s^{CH_2}$ band positions. The $\nu_a^{CH_2}$ bands for the **C*n*C2**, **C*n*C3**, and **t-C*n*** SAMs appeared at 2924, 2925, and 2926 cm^{-1}, respectively. The observation of such small differences in the $\nu_a^{CH_2}$ band positions for the loosely packed SAMs is surprising, given the large differences in the contact angles of hexadecane shown in Figure 5a: $\Delta \sim 12°$ for the **C*n*C2** and **C*n*C3** SAMs and $\Delta \sim 6°$ for the **C*n*C3** and **t-C*n*** SAMs. As noted previously,[28] the $\nu_a^{CH_2}$ band position is relatively insensitive to small differences

(45) Ulman, A. *An Introduction to Ultrathin Organic Films*; Academic: Boston, 1991.
(46) *Characterization of Organic Thin Films*; Ulman, A., Ed.; Butterworth-Heinemann: Boston, 1995.
(47) Colorado, R., Jr.; Lee, T. R. *J. Phys. Org. Chem.* **2000**, *13*, 796.
(48) Sheen, C. W.; Shi, J. X.; Maartensson, J.; Parikh, A. N.; Allara, D. L. *J. Am. Chem. Soc.* **1992**, *114*, 1514.
(49) Snyder, R. G.; Hsu, S. L.; Krimm, S. *Spectrochim. Acta* **1978**, *34A*, 395.
(50) MacPhail, R. A.; Strauss, H. L.; Snyder, R. G.; Elliger, C. A. *J. Phys. Chem.* **1984**, *88*, 334.
(51) Snyder, R. G.; Strauss, H. L.; Elliger, C. A. *J. Phys. Chem.* **1982**, *86*, 5145.
(52) Bensebaa, F.; Ellis, T. H.; Badia, A.; Lennox, R. B. *J. Vac. Sci. Technol., A* **1995**, *13*, 1331.
(53) Bensebaa, F.; Ellis, T. H.; Badia, A.; Lennox, R. B. *Langmuir* **1998**, *14*, 2361.

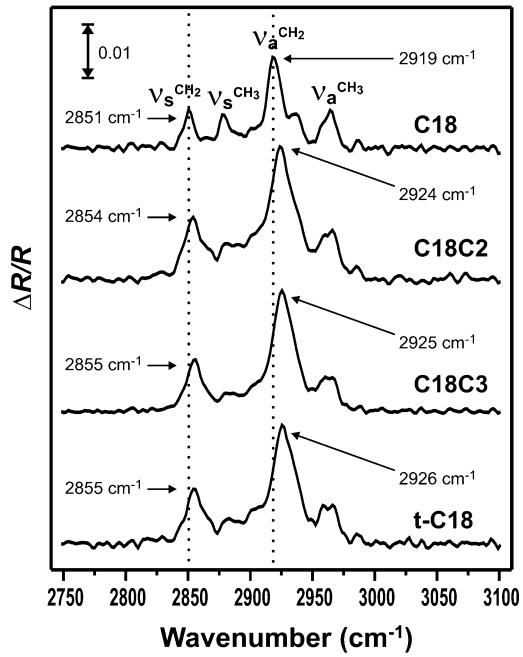

Figure 6. C−H stretching region of the PM-IRRAS spectra of SAMs derived from octadecanethiol (**C18**), 2-hexadecylpropane-1,3-dithiol (**C18C2**), 2-hexadecyl-2-methylpropane-1,3-dithiol (**C18C3**), and 1,1,1-tris(mercaptomethyl)heptadecane (**t-C18**).

Table 2. Band Positions of the Methylene Antisymmetric Stretch ($\nu_a^{CH_2}$) and the Methylene Symmetric Stretch ($\nu_s^{CH_2}$) for SAMs Generated from the Indicated Adsorbates[a]

adsorbate	C12	C14	C16	C18
	Methylene Antisymmetric Stretch ($\nu_a^{CH_2}$)			
C*n*	2921.0	2919.0	2919.0	2918.5
C*n*C2	2924.1	2924.0	2924.1	2924.2
C*n*C3	2925.2	2925.1	2925.2	2925.4
t-C*n*	2925.8	2926.0	2925.9	2926.0
	Methylene Symmetric Stretch ($\nu_s^{CH_2}$)			
C*n*	2851.2	2850.7	2850.8	2850.7
C*n*C2	2855.2	2854.2	2853.9	2854.0
C*n*C3	2855.3	2854.7	2854.7	2855.4
t-C*n*	2855.8	2855.6	2855.2	2855.0

[a] The $\nu_a^{CH_2}$ and $\nu_s^{CH_2}$ band positions were obtained from at least three independent experiments and were reproducible within ±1 cm^{-1} of those reported.

in the degree of conformational order of liquidlike SAMs. Despite this limitation, the observed positions of the $\nu_a^{CH_2}$ bands suggest that the conformational order of the SAMs decreases in the following order: **C*n*** ≫ **C*n*C2** > **C*n*C3** > **t-C*n***. This conclusion is consistent with the observed $\nu_s^{CH_2}$ band positions, which appeared at 2854, 2855, and 2855 cm^{-1} for the **C*n*C2**, **C*n*C3**, and **t-C*n*** SAMs, respectively, indicating a liquidlike conformational order for all three types of SAMs.

It is difficult to evaluate the position of the methyl symmetric band ($\nu_s^{CH_3}$) because the intensity of the peak decreases markedly with decreasing conformational order (Figure 6). Instead of the peak position, the relative intensity of the $\nu_s^{CH_3}$ band can provide qualitative information regarding the degree of conformational order. According to the schematic model of the normal alkanethiol SAMs (**C*n***), the $\nu_s^{CH_3}$ transition dipole is oriented nearly parallel to the surface normal (especially in the even-numbered SAMs),[52,53] leading to a strong absorption for the mode. In loosely packed SAMs, however, the presence of gauche defects might be expected to randomize the orientation of methyl groups and thus diminish the intensity of the $\nu_s^{CH_3}$ bands.[52,53] Indeed, Figure 6 shows that the loosely packed SAMs (**C*n*C2**, **C*n*C3**, and **t-C*n***) exhibited substantially diminished $\nu_s^{CH_3}$ peak intensities compared to the densely packed analogues (**C*n***). Unsurprisingly, the intensity of the methylene antisymmetric bands ($\nu_a^{CH_2}$) shows the opposite effect. In the highly ordered **C*n*** SAMs, the $\nu_a^{CH_2}$ transition dipole is oriented nearly parallel to the surface. In the loosely packed SAMs, the random orientation of the methylene groups will likely lead to some $\nu_a^{CH_2}$ transition dipoles oriented along the surface normal, enhancing the intensity of the $\nu_a^{CH_2}$ bands. Figure 6 shows this trend. Given, however, that the quantitative analysis of PM-IRRAS signals is more complex than that of IRRAS signals,[54,55] any conclusions drawn from peak intensities should be verified by additional analysis.

The $\nu_a^{CH_3}$ bands consist of in-plane and out-of-plane modes, and the relative intensities of these modes vary with the degree of conformational order.[53] Furthermore, the $\nu_a^{CH_3}$ peak position is known to be insensitive to the conformational order of the alkyl chains in SAMs.[44] For example, normal alkanethiol SAMs (**C*n***, $n = 3-21$) exhibit $\nu_a^{CH_3}$ in-plane modes at 2965−2966 cm^{-1} regardless of the degree of conformational order.[44] Likewise, for all of the SAMs examined in this research, the $\nu_a^{CH_3}$ in-plane modes are observed at 2965−2966 cm^{-1}. The $\nu_a^{CH_3}$ out-of-plane mode has been reported to appear at 2956 and 2957 cm^{-1} for crystalline *n*-docosanethiol and liquid *n*-octanethiol, respectively. As shown in Figure 6, however, it is impossible to track the precise position of the $\nu_a^{CH_3}$ out-of-plane mode. Instead, we suggest that the relative intensity of the $\nu_a^{CH_3}$ in-plane and out-of-plane modes (i.e., $\nu_a^{CH_3}$ in-plane/$\nu_a^{CH_3}$ out-of-plane) can provide qualitative insight regarding the conformational order of the SAMs. In most surface infrared spectra, the methyl antisymmetric out-of-plane modes are masked by the in-plane modes due to the orientation of the former mode with respect to the surface.[44] In loosely packed SAMs, however, the random orientation of the methyl groups leads to a substantial number of the $\nu_a^{CH_3}$ out-of-plane modes oriented along the surface normal. In Figure 6, the **C18** SAM exhibits what appears to be a predominant $\nu_a^{CH_3}$ in-plane mode at 2965 cm^{-1}, while the corresponding loosely packed SAMs (**C18C2**, **C18C3**, and ***t*-C18**) exhibit both in-plane and out-of-plane modes at 2966 and ∼2958 cm^{-1}, respectively.

As a whole, the PM-IRRAS spectra support the relative packing densities of the SAMs inferred from the ellipsometry and contact angle measurements. Furthermore, the PM-IRRAS data offer a direct evaluation of the conformational order of the SAMs. The peak position and bandwidth of C−H stretches are, however, relatively insensitive to small changes in conformational order for highly disordered, liquidlike SAMs.[28]

Packing Density. In XPS, the binding energy (E_B) of an electron in an atom is a function of the type of atom and its environment.[37] Thus, bond formation between atoms can be evaluated by monitoring the binding energy shift because bonding can change the electron distribution of the atom of interest. Another factor that influences binding energy is the electrical conductivity of the sample.[37] For normal alkanethiol SAMs (**C*n***), it has been reported that the binding energy of the C_{1s} photoelectron shifts to a lower value when the alkyl chain length decreases.[17,40] Assuming that the nature of gold−thiolate bonds is unaffected by changing the length of alkyl chains,

(54) Buffeteau, T.; Desbat, B.; Turlet, J. M. *Appl. Spectrosc.* **1991**, *45*, 380.
(55) Buffeteau, T.; Desbat, B.; Blaudez, D.; Turlet, J. M. *Appl. Spectrosc.* **2000**, *54*, 1646.

Table 3. XPS Binding Energies (eV), Integrated Photoelectron Intensities (counts), Relative Chain Densities, and S_{2p}/Au_{4f} Peak Intensity Ratios of SAMs Derived from the Indicated Adsorbates[a]

adsorbate	C_{1s} (eV)	S_{2p} (eV)	Au_{4f} (counts)	C_{1s} (counts)	S_{2p} (counts)	chain density from Au_{4f} (%)	chain density from C_{1s} (%)	S_{2p}/Au_{4f}
C16	285.0	162.0	93500	11035	597	100	100	0.0064
C16C2	284.8	162.0	110435	7783	814	64	66	0.0074
C16C3	284.9	162.1	113920	7207	864	56	58	0.0076
t-C16	284.6	162.0	116571	6697	984	51	53	0.0084
C18	285.1	162.0	86359	11759	549	100	100	0.0064
C18C2	284.9	162.0	104490	8464	801	65	65	0.0077
C18C3	284.9	161.8	109034	7945	848	57	58	0.0078
t-C18	284.7	162.0	111768	7392	951	51	53	0.0085

[a] We report average values of three independent measurements. The binding energies were referenced to $Au_{4f\ 7/2}$ at 84.0 eV. Although the absolute peak areas varied from sample to sample, the calculated chain densities from Au_{4f} were always within ±2%, and those from C_{1s} were within ±3% of those reported.

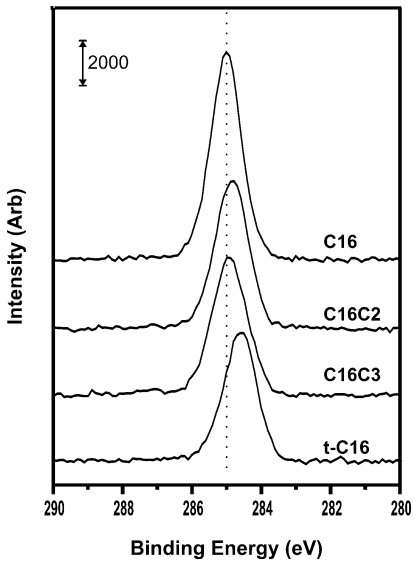

Figure 7. XPS spectra of the C_{1s} region for SAMs derived from hexadecanethiol (**C16**), 2-tetradecylpropane-1,3-dithiol (**C16C2**), 2-methyl-2-tetradecylpropane-1,3-dithiol (**C16C3**), and 1,1,1-tris(mercaptomethyl)pentadecane (**t-C16**).

the binding energy shift has been rationalized on the basis of changes in the polarizability of the SAMs. Likewise, the C_{1s} peak position for the **C18** SAM has been reported to shift to a lower energy when the SAM is partially decomposed.[56] It was proposed that the positive charges generated by photoelectron emission can be more easily discharged by the partially decomposed loosely packed SAMs than by the densely packed analogues because the loosely packed SAMs act as poor insulators. The C_{1s} binding energy can therefore be used as a rough measure of the thickness and/or coverage of SAMs.

Figure 7 and Table 3 show a small but reproducible shift of the C_{1s} peak to lower binding energy for the **C*n*C2** and **C*n*C3** SAMs when compared to the densely packed **C*n*** SAMs ($\Delta E_B \sim 0.2$ eV). The shift to lower binding energy for the **t-C*n*** SAMs is notably larger ($\Delta E_B = 0.4$ eV). From the observed shifts, the relative packing density and film thickness of the SAMs can be estimated to be **C*n*** > **C*n*C2** ~ **C*n*C3** > **t-C*n***, which is roughly consistent with the analyses described above. We note, however, that the C_{1s} binding energy can be influenced by other factors, including the orientation of alkyl chains.[57]

We have found that the relative packing density of loosely packed SAMs can be quantitatively evaluated by analyzing the Au_{4f} peak intensities,[23,28] because the Au_{4f} peak is attenuated by overlying adsorbates, and thus the intensity of the peak is reversely proportional to the amount and/or thickness of the adsorbed overlayer. Consequently, the packing densities of alkyl chains in loosely packed SAMs relative to that in densely packed **C*n*** SAMs can be obtained by comparing their attenuated Au_{4f} peak intensities, because the packing density and thickness of **C*n*** SAMs are precisely known. Analysis of the composition of SAMs in a quantitative manner requires knowledge of the absolute value of the attenuation length (λ).[58–60] First, we monitored the attenuation of the $Au_{4f\ 7/2}$ peak in a series of normal alkanethiol SAMs (**C10**, **C12**, **C14**, **C16**, and **C18**). The attenuated Au_{4f} signal is described by eq 1:[58]

$$\ln Au_n = -nd/(\lambda \sin \theta) + \text{constant} \qquad (1)$$

where Au_n is the intensity of the Au_{4f} signal attenuated by an n carbon monolayer, d is the thickness of the SAM per methylene unit, λ is the attenuation length, and θ is the takeoff angle. The contribution of sulfur to the attenuation of the gold signal must also be considered and was assumed to be equivalent to attenuation by 1.5 carbon atoms.[7] A least-squares analysis of the attenuated gold signals obtained from the series of **C*n*** SAMs yielded an attenuation length of 41 Å, which is in good agreement with previously reported values.[23,28,58] Next, we measured the attenuated gold signals of the loosely packed SAMs and then derived an "effective" number of carbon atoms per adsorbate from the signals using the calibration curve constructed from the **C*n*** SAMs. Finally, a direct comparison of the "effective" number of carbon atoms per adsorbate with the actual stoichiometric number of carbon atoms per adsorbate in the loosely packed SAMs gave the alkyl chain density of the SAMs relative to that of the densely packed **C*n*** SAMs. As shown in Table 3, the **C*n*C2**, **C*n*C3**, and **t-C*n*** SAMs were found to possess 65, 57, and 51%, respectively, of alkyl chain density relative to the corresponding **C*n*** SAMs (normalized to 100% packing density).

The relative chain density can also be derived from the C_{1s} peak intensities.[23,28] In this approach, we constructed a calibration curve using the C_{1s} peak intensities and the actual stoichiometric number of carbon atoms per adsorbate. In this case, sulfur cannot influence the C_{1s} peak intensity because all of the carbon atoms lie above the sulfur atoms. This approach afforded the same trend obtained from the attenuated gold signals (Table 3). As

(56) Ishida, T.; Hara, M.; Kojima, I.; Tsuneda, S.; Nishida, N.; Sasabe, H.; Knoll, W. *Langmuir* **1998**, *14*, 2092.
(57) Himmel, H. J.; Woell, C.; Gerlach, R.; Polanski, G.; Rubahn, H. G. *Langmuir* **1997**, *13*, 602.
(58) Bain, C. D.; Whitesides, G. M. *J. Phys. Chem.* **1989**, *93*, 1670.
(59) Colorado, R., Jr.; Lee, T. R. *J. Phys. Chem. B* **2003**, *107*, 10216.
(60) We define the term "attenuation length" as the thickness of the monolayer film that is required to reduce the flux of the emitted photoelectrons by 1/e.

a whole, quantitative analyses by XPS demonstrated that the packing densities decrease in the order **C*n*** ≫ **C*n*C2** > **C*n*C3** > **t-C*n***. The results provide strong evidence that the low film thicknesses, enhanced wettabilities, and decreased degree of conformational order of loosely packed SAMs arise from the loose packing of the alkyl chains. Furthermore, the results suggest that the alkyl chain density in hydrocarbon SAMs can be precisely varied between 50% and 65% by selecting an appropriate chelating adsorbate.

The XPS data in Table 3 can also be used to estimate the relative density of thiolates on the surface, although the low signal-to-noise ratio of the S_{2p} region hinders precise integration of the peaks. According to the XPS spectra in Figure 3 and previous work,[23,28] we infer that all of the thiolates in the SAMs examined in this paper are completely bound (vide supra). Therefore, the surface density of the thiolates can be estimated from the ratio of the sulfur-to-gold signal intensities (S_{2p}/Au_{4f}).[61] As shown in Table 3, the densities of thiolates in loosely packed SAMs generated from the bidentate adsorbates (**C*n*C2** and **C*n*C3**) are indistinguishable from each other and ~20% greater than those in normal alkanethiol SAMs (**C*n***). In contrast, the surface densities of thiolates in the SAMs derived from the tridentate adsorbates (**t-C*n***) are even higher (~30% greater than the **C*n*** SAMs).

Despite these data, we are presently unable to provide an accurate structural model for the binding of loosely packed SAMs on gold. Given, however, the increased sulfur densities in loosely packed SAMs, we can safely assume that the average sulfur−sulfur spacing is substantially smaller than that of densely packed **C*n*** SAMs (5 Å).[33,34] Thus, some of the thiolate groups must occupy sites other than the 3-fold hollows on Au(111).

Preliminary Evaluation of the Thermal Stability of SAMs Generated from t-C*n*. Recently, we reported an enhanced thermal stability for SAMs generated from the bidentate chelating adsorbates (**C*n*C2**) when compared to SAMs generated from normal alkanethiols (**C*n***).[26] The enhanced stability of the **C*n*C2** SAMs was rationalized on the basis of the chelate effect and the ring strain generated in the formation of intramolecular cyclic disulfide desorption products. Given this background, we anticipated that the tridentate chelating adsorbates (**t-C*n***) would form monolayers on gold that were even more stable than the analogous bidentate chelating adsorbates (**C*n*C2** and **C*n*C3**). To test this hypothesis, we examined SAM desorption in decalin at elevated temperatures using a previously established protocol.[26] Decalin was chosen due to its high boiling point (189−191 °C) and its ability to minimize possible intercalation into the decomposed SAMs.[26,62] The preformed SAMs were immersed in decalin at temperatures ranging from 70 to 110 °C. Upon removal from the decalin solution at selected intervals of time, the SAMs were rinsed thoroughly with ethanol and blown dry with a stream of ultrapure nitrogen. The fraction of SAM remaining on the surface was then measured by ellipsometry. These preliminary trials showed the relative stabilities of the SAMs are as follows: **t-C*n*** > **C*n*C2** ~ **C*n*C3** > **C*n***. For example, an experiment conducted at 110 °C showed that after 3 min, ~33% of the SAM derived from **t-C18** and ~20% of the SAMs derived from **C18C2** and **C18C3** remained on the surface, while the SAM derived from **C18** decomposed almost completely after only 1 min. These preliminary results suggest that SAMs derived from the tridentate adsorbates (**t-C*n***) are more thermally stable than those derived from the bidentate adsorbates (**C*n*C2** and **C*n*C3**), which are themselves more stable than those derived from normal alkanethiols (**C*n***). We are currently exploring the relative stabilities of the SAMs in a more quantitative fashion to evaluate the importance of the chelate effect in dictating the thermal stabilities of SAMs on gold.

Conclusions

A series of new tridentate chelating adsorbates were synthesized and used to prepare loosely packed SAMs on gold. Characterization of the SAMs revealed that the tridentate **t-C*n*** adsorbates generate uniform monolayer films having low densities of alkyl chains. The data were compared with those obtained on SAMs generated from bidentate chelating alkanedithiols and normal alkanethiols. The comparison showed that the **t-C*n*** SAMs possess lower packing densities of alkyl chains than the **C*n***, **C*n*C2**, and **C*n*C3** SAMs. Correspondingly, the SAMs derived from **t-C*n*** are the least conformationally ordered and most tilted from the surface normal on average. The trends in packing density and conformational order of the SAMs were observed to decrease as follows: **C*n*** ≫ **C*n*C2** > **C*n*C3** > **t-C*n***. Furthermore, a preliminary evaluation of thermal stability revealed that the **t-C*n*** SAMs are more stable than those derived from **C*n***, **C*n*C2**, and **C*n*C3**, apparently due to an enhanced chelate effect. As a whole, the results demonstrate that the packing density, conformational order, and thermal stability of SAMs on gold can be precisely controlled by tailoring the structures of chelating alkanethiol adsorbates.

Acknowledgment. The Robert A. Welch Foundation (Grant No. E-1320), the National Science Foundation (NIRT Award ECS-0404308), and the Texas Advanced Research Program (003652-0307-2001) provided generous support for this research.

Supporting Information Available: ^{1}H and ^{13}C NMR spectra of 1,1,1-tris(mercaptomethyl)alkanes. This material is available free of charge via the Internet at http://pubs.acs.org.

LA0475573

(61) This method of estimation assumes that the attenuation length of S_{2p} photoelectrons is the same as that of Au_{4f} photoelectrons in hydrocarbon SAMs. An alternative method in which the absolute S_{2p} photoelectron intensities are compared directly is less reliable because the S_{2p} intensities are attenuated by different overlayers for each of the different samples.

(62) Jennings, G. K.; Laibinis, P. E. *Langmuir* **1996**, *12*, 6173.